Fault diagnosis of Planetary Gearbox under Time-varying Speed Conditions Based on Convolutional Neural Network

Chuan Zhao
School of Electromechanical Engineering
North China Institute of Aerospace Engineering
Langfang, China
zhcuhh@163.com

Zhipeng Feng
School of Mechanical Engineering
University of Science and Technology Beijing
Beijing, China
fengzp@ustb.edu.cn

***Abstract*—Fault diagnosis of planetary gearboxes under time-varying running conditions is a highly challenging topic due to the frequency complexity and time variability of vibration signals. Conventional statistics are unsuitable to describe such nonstationary signals. Time-frequency analysis can extract the frequency components of nonstationary signals and their time variability, but expertise knowledge is required. In order to address the issue of fault diagnosis under time-varying conditions, an intelligent fault diagnosis method is proposed, by exploiting the capability of convolutional neural networks in image processing. Firstly, the time-frequency representations of signals are constructed, and are treated as images. Such images are compressed, and their RGB weighted averages are used for further image processing. Secondly, a convolutional neural network (CNN) is established for intelligent fault pattern identification. Convolutional calculation is exploited to adaptively extract the features of time-frequency images, and a multi-layer perceptron network is trained to diagnose planetary gearbox faults under time-varying speeds. The proposed method is validated experimentally.**

Keywords- convolutional neural work; fault diagnosis; planetary gearbox; time-varying speed

I. INTRODUCTION

Planetary gearboxes are widely used in many sorts of machinery for their merits of large transmission ratio, excellent load-bearing capacity in a compact structure. Under poor operating circumstances and alternating heavy loads, the key component, such as sun, planet and ring gears, are prone to damage. Once damage occurs, it will develop gradually, and eventually lead to breakdown of entire machine. Therefore, planetary gearbox fault diagnosis is an important topic.

In practice, planetary gearboxes often run under nonstationary conditions. In this case, fault diagnosis is a highly challenging issue. Planetary gearbox fault diagnosis relies on detecting fault characteristic frequencies and monitoring their magnitude changes. However, the unique structure and intricate kinematics of planetary gearboxes lead to complex vibration signals, which makes it difficult to identify fault characteristic frequencies. Recently, many researchers have made contributions to planetary gearbox fault diagnosis in perspective of dynamic analysis and signal analysis [1-3]. Nevertheless, most of reported studies assume that planetary gearboxes run under stationary conditions, which means fault characteristic frequencies are constant. However, in practice, the running speed and/or load of planetary gearboxes are usually time-varying. This leads to nonstationary vibration signals and time-varying fault characteristic frequencies, and further adds difficulty to fault diagnosis.

For nonstationary signals, time-frequency analysis has been demonstrated effective to extract frequency contents and their time variability. Well-known time-frequency analysis methods include short time Fourier transform (STFT), wavelet transform, Wigner-Ville distribution, and empirical mode decomposition, etc. However, for fault diagnosis of planetary gearbox under nonstationary conditions, they suffer from poor time-frequency resolution and/or pseudo interferences, which hinders fault features extraction. In order to overcome this difficulty, researchers have made some improvements [4-10]. For example, Feng et al. [4,5] studied time-frequency analysis methods based on iterative generalized demodulation and synchrosqueezing transform, and effectively extract time-varying fault frequencies of planetary gearboxes under nonstationary conditions. Chen et al. [6,7] proposed order spectrum analysis methods based on amplitude demodulation, frequency demodulation, and iterative generalized time-frequency reassignment for planetary gearbox fault diagnosis under nonstationary conditions. Besides, Chen et al. [8] studied the time-frequency features of planetary gearbox torsional vibration signals under nonstationary condition. Wang et al. [8] extracted the entropy feature of vibration signal phase angle for failure detection of planetary gearbox under nonstationary condition. Guan et al. [9] mapped the original nonstationary signal into a smooth signal in angle domain, then extracted planetary gearbox fault features through synchrosqueezing transform. Hu et al. [10] used high-order synchrosqueezing transform to reveal the time-frequency features of planetary gearbox fault vibration signals under nonstationary conditions. The above publications contribute to planetary gearbox fault diagnosis under nonstationary conditions, but most of the work involve expert's participation and rely on data analyst's

This work is supported by National Natural Science Foundation of China (51875034, 51475038) and doctoral research startup fund (BKY-2018-05)

978-1-7281-0860-5/19/$31.00 ©2019 IEEE

knowledge to identify fault characteristic frequencies manually. The subjective factors may affect the fault diagnosis accuracy.

Intelligent fault diagnosis provides an approach to avoid subject factors. In some latest reports, intelligent fault diagnosis strategies have been proposed for intelligent fault identification of planetary gearboxes [11-13]. Liu et al. [11] decomposed the signal into intrinsic mode functions (IMF) with EEMD and investigated the dependence between the raw signal and each IMF by Archimedean Copulas, applied the associated indicators to form a dependence-based feature vector, and classified gear faults by a multi-class support vector machine. Li et al. [12] used modified hierarchical permutation entropy (AMMF) to extract fault features, and employed a binary tree support vector machine to identify gear fault patterns. Wang et al. [13] combined generative adversarial networks (GAN) and stacked denoising autoencoders (SDAE) to generate new samples for expanding the sample size and automatically extract effective fault features, and discriminated their authenticity and fault categories. However, most of intelligent diagnosis methods use 1D indices as input features. These 1D indices are usually statistical indicators of signals under stationarity assumption, and are unsuited for nonstationary conditions. Therefore, intelligent fault diagnosis of planetary gearboxes under nonstationary conditions is still a challenging topic.

Recently, convolutional neural network (CNN) has the merit of mining representative information and sensitive features from raw data, and has been demonstrated an effective approach for intelligent fault diagnosis of machinery. Jing et al. [14] used a convolutional neural network to extract features automatically from vibration signals for gearbox fault diagnosis. Zhao et al. [15] acquired three different types of dynamic encoder information from the raw position sequence and constructed multivariate encoder information by data fusion, and diagnosed faults using a convolutional neural network. However, most of these publications use 1D indicators as inputs to CNN, and therefore focus on constant conditions only. The capability of CNN in 2D image processing has not been well exploited in machinery fault diagnosis field.

In this paper, we propose an intelligent method to address the issue of planetary gearbox fault diagnosis under nonstationary conditions, by exploiting both the capability of time-frequency analysis in nonstationary signal processing and that of CNN in image pattern identification. We extract time-varying fault features through time-frequency analysis, solving the problem due to nonstationary conditions. Then, we treat time-frequency representations as images, input them to CNN, realizing intelligent fault pattern identification. This framework is robust to the time-frequency resolution and possible pseudo interferences, and therefore any time-frequency analysis methods are applicable. Moreover, it can be generalized to fault diagnosis of any machinery under nonstationary conditions.

The remainder of this paper is organized as follows. In Section 2, fundamentals of CNN are introduced. In Section 3, a CNN-based intelligent diagnosis method is presented. Next, it is validated using a planetary gearbox experimental dataset in Section 4. Finally, conclusions are drawn in Section 5.

II. AN INTRODUCTION OF CONVOLUTIONAL NEURAL NETWORK

A. *Convolutional computation and feature learning*

Convolutional computation plays an important role in analysis mathematics which consists of continuous convolution and discrete convolution. Convolutional computation involved in convolutional neural network is the latter, and the computational formulation is presented in (1), where i denotes the ith discrete data point in a series while n denotes an integral time shift. In another word, convolutional computation can be regarded as a mathematical operator to generate a third function y for measuring product of function x and h which has been reversed and time shifted.

$$y(n)=\sum_{i=-\infty}^{\infty}x(i)\,h(n-i)=x(n)*h(n) \tag{1}$$

However, in practical application of convolutional neural network, the input is generally image. Next, a description of two-dimensional convolutional computation in detail is given. For example, suppose the input data is $X\in R^{5\times6}$, where 5 and 6 are dimensions of the data, and another operator $H\in R^{3\times3}$, called convolution kernel or convolution filter, is utilized to carry out the computation with stride 1. The concrete instances and computation process are presented in Fig. 1 and Fig. 2. From Fig.2, we can see that size of the convolution kernel determines the size of sub-field participated in the computation while elements in the sub-field determines contributions of the input data to the results called features.

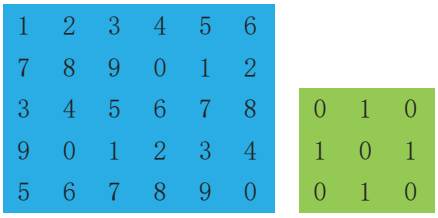

(a) (b)

Fig. 1 Two-dimensional input data and convention kernel: (a) Input X (b) convention kernel H

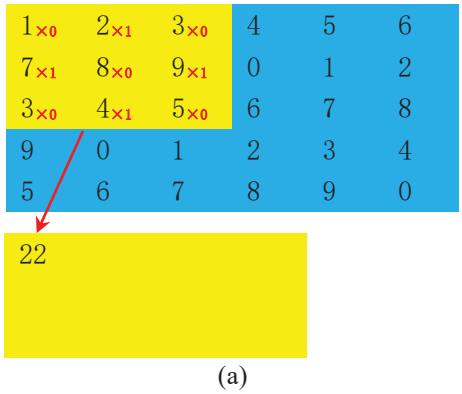

(a)

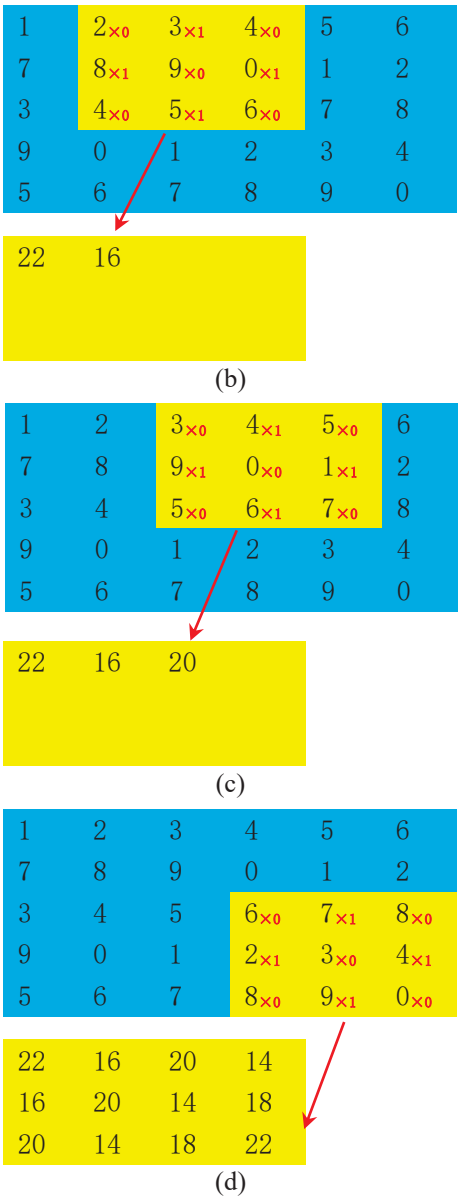

Fig. 2 Two-dimensional convolution computation process: (a) The first convolution operation and the feature (b) the second convolution operation and the feature (c) the third convolution operation and the feature (d) the twelfth convolution operation and the feature

Generally, in the process of traditional fault diagnosis of rotating machine, features are first constructed and extracted with expertise from raw signal, then further used to train models, and finally classified for detecting faulty components automatically. In recent years, feature learning technology replaces feature engineering gradually, where features are hand-crafted with expertise for specific task. Different from feature engineering, feature learning technology outputs a new representation of raw signal, which should be better for classification than raw input data by learning a transformation or transformations of raw data with learnable parameters.

In our study, a concrete convolution kernel is given in Fig.1 (b) for a brief explanation of convolution computation, elements of which originally should be unknown, and required to be trained in practical application of CNN. The trained convolution kernel is finally used for learning optimal features.

B. *Multi-layer perceptron*

After feature learning, features are used to train models, most of which derive from multi-layer perceptron (MLP) neural network structure and classified for fault identification. As a feedforward neural network, MLP consists of input layer, hidden layer or layers, and output layer. A schematic structure of MLP is presented in Fig. 3, where x_1 denotes the data input in the first neuron of input layer, ω_{11}^2 denotes the weight value from first neuron in the first layer to first neuron in the second layer, and y_1^2 denotes the output of first neuron in the second layer. In a MLP, neurons in the same layer are independent, while neurons in adjacent layers are fully-connected. The data are input to the input layer and transmitted along the array direction. Each neuron in the latter layer will receive the weighted value of all the neurons in a former layer. The relationship is presented in (2), where l means the lth layer, m denotes the mth neuron in lth layer, k is the number of neurons in l-1th layer, i is the ith neuro in it, b is a bias, and f denotes an active function. Here f can be sigmoid, tanh, and relu, which are presented in (3) - (5).

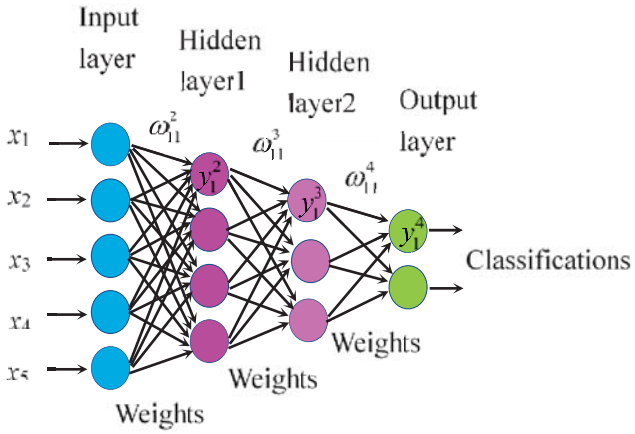

Fig. 3. A schematic structure of MLP

$$y_m^l = f\left(\sum_{i=1}^{k} \omega_{im}^{l-1} \times y_i^{l-1} + b_m^l\right) \tag{2}$$

$$s(x) = \frac{1}{1+e^{-x}} \tag{3}$$

$$\tanh x = \frac{\sinh x}{\cosh x} = \frac{e^x - e^{-x}}{e^x - e^{-x}} \tag{4}$$

$$f(x) = \max(0, x) \tag{5}$$

C. *Convolutional neural network*

Much research has indicated that CNN works very well in image identification and classification [16]. In order to adaptively extract features of time-frequency map of analyzed signal collected from planetary gearbox under variable speed condition, a CNN-based model is proposed. The primary

model of CNN is called neurocognitive machine, which is a biophysical model inspired by the neural mechanism of the visual system. In fact, CNN can be regarded as a special multi-layer perceptron or feed-forward neural network, which has properties of local connection and weight sharing. Generally, a CNN consists of input layer, convolutional layer, pooling layer, fully-connected layer and output layer, which are presented in Fig.4.

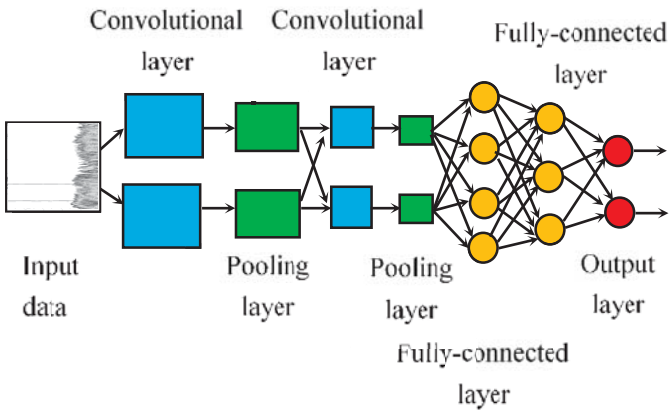

Fig. 4. A schematic structure of CNN (with two kernels)

Compared with Fig.3, a CNN can be presented as a combined model with part of convolutional calculation and a MLP. Through convolutional calculation carried out by several combined layers, i.e. convolutional layers and pooling layers, features of images are adaptively extracted and dimension-reduced. Then, the MLP will further extract dimension-reduced features layer by layer for more brief representation of the original input data and classify the new features. Descriptions of each layer in detail are as follows:

1) Input layer: for image input, the input layer can process image pixels directly.

2) Convolutional layer: in the convolutional layer, each rectangular block is called a feature map. From the example of a two-dimensional convolutional operation presented in Fig.2, it can be seen that a feature map corresponds to a feature matrix obtained by convolutional operation, and the number of neurons in a feature map is the same as that of elements in the matrix. The sub-block of input data or a feature map, involved in one convolutional calculation, is called a partial receptive field, while the weighted matrix is called a convolutional kernel, which is presented in Fig.1. Besides, each feature map corresponds to only one convolutional kernel, and a single neuron in a feature map corresponds to a local receptive field, and all neurons in a feature map share the weights in the kernel. The weights of a kernel are generally unknown and needed to be initialized and trained. However, sometimes the convolutional kernel can also be given with fixed weights, such as a Gabor filter [17]. The convolutional layer extracts feature of input data through convolutional calculation, and different kernels focus on different features. With more convolution kernels, richer features of input data can be extracted.

3) Pooling layer: it is also called down-sampling layer, and has several feature maps, which have one-to-one correspondence to the former feature maps. The neurons in feature maps of pooling layer are connected to corresponding local receptive field of former layer, and the receptive fields do not overlap. The main purpose of this layer is to reduce the feature dimension without losing feature information and improve the efficiency of the network. The commonly used pooling methods mainly include maximum pooling, i.e. extracting the maximum value in the local receptive field, mean value pooling, i.e. averaging all the elements in the local receptive field, and randomly pooling [18]. In a CNN model, the convolutional layer and pooling layer are usually regarded as a unit and called combined convolutional layer. A CNN model can have a few of combined convolutional layers, and the combined convolutional layers can be full-connected or not. With more combined convolutional layers, the more abstract features can be obtained.

4) Fully-connected layer: Corresponding to the hidden layer of a MLP, a CNN model may include one or more fully-connected layers or may not include any fully-connected layer. Each neuron in the fully-connected layer is connected to all neurons in the previous layer, so that local information with class discrimination in the pooling layer can be integrated. The active function is generally sigmoid.

5) Output layer: The values of the last layer of fully-connected layer are transmitted to the output layer, and the number of neurons in output layer is set according to a specific task.

III. CNN-BASED MODELS OF INTELLIGENT DIAGNOSIS

For the fault diagnosis of planetary gearbox under variable speed condition, the intelligent diagnosis model based on CNN is shown in Fig. 5. The steps are as follows:

1) Acquire vibration signals under variable speed conditions and divide the signals into training samples and test samples.

2) The short time Fourier transform method is used to obtain the time-frequency map of the analyzed sample signal and compress the time-frequency into a small size.

3) Transform the RGB image into a gray one and use the weighted average algorithm to calculate the weighted average of the R, G, and B components, and calculate them according to (6).

$$Ave = 0.2989R + 0.5870G + 0.1140B \tag{6}$$

4) Input the time-frequency grayscale image of training samples into the convolutional neural network model and train the network model parameters. The model structure can refer to the convolutional neural network structure in the Deep Learn Toolbox open source library in [19].

5) Testing samples are used to test the model, and faults of planetary gearbox under variable speed condition are diagnosed.

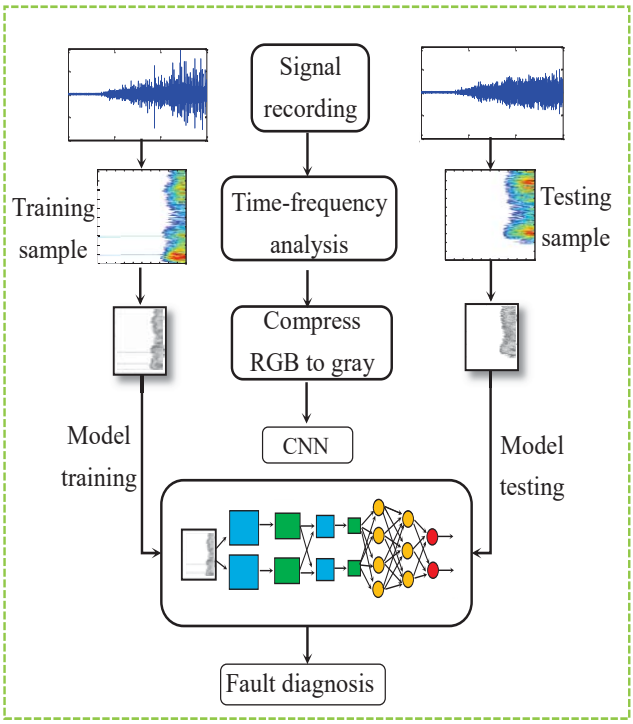

Fig. 5 Flow chart of CNN-based intelligent diagnosis model

IV. VALIDATION OF THE PROPOSED MODEL

A. *Experimental configuration*

In this section, the proposed method is validated by lab experimental data set under variable speed. Fig.6 presents the experimental set-up. The motor is connected to the input shaft through a torque-speed sensor to drive the sun gear. The torque-speed sensor is used to measure the torsional vibration and speed. The output shaft of the planetary gearbox is connected to the planet carrier and applied a load provided by an electromagnetic brake. Several acceleration sensors are mounted on the base of planetary gearbox and top of planetary gearbox case for measuring vibrations. The configuration parameters of the planetary gearbox are listed in Table 1, which can help to derive relationships between sun gear rotating frequency and characteristic frequencies as listed in Table 2. Fig.7 shows the figures of gears with manual damage for simulation. Therefore, we carried out four cases of running conditions i.e. (1) healthy baseline case with all gears healthy, (2) sun gear fault case with a local fault on the sun gear alone, (3) planet gear fault case with a local fault on one of the planet gears alone, and (4) ring gear fault case with a local fault on the ring gear alone. For each case, the motor speed varies from 0-25Hz in a period of 15 seconds which includes 3 seconds for start delay, 10 seconds for speeding up from 0 to 25Hz and 2 seconds for operating at 25Hz and the experiment will be repeated for 50 times. In this study, we analyze signal from sensor on the top of the gearbox and the vibration signals are collected at a sampling rate of 20480Hz. Therefore, we will obtain 200 data sets for all the cases with 307200 data points in each set. For convenience, resample the signal at a new sampling rate of 1024 Hz, and only the points collected from the 3th second to the 13th second will be utilized for analysis in each set. Thus, a final analyzed single set contains 10240 points. Divide each set into 10 segments, which are coded from 1 to 10, and put segments from 1 to 5 into a sample, segments from 2 to 6 into a sample, and so on, then 6 samples are available for each set of signals. Then, we can obtain 300 samples for each state, while each sample contains 5120 data points. Select 150 samples among them randomly for training, others for testing. Finally, the training samples for four states are totally 600, while testing samples are 600. The signal waveform, Fourier spectrum for each case are shown in Fig. 8. The speed curve is presented in Fig.9.

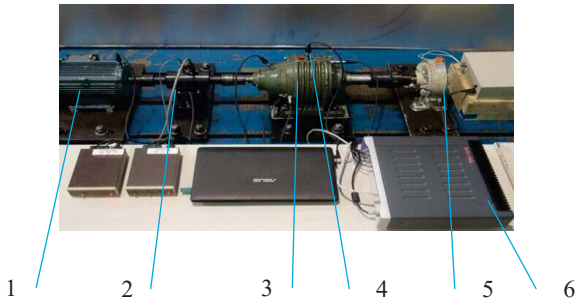

1-drive motor, 2-tachometor, 3-planetary gearbox, 4-accelerometer, 5-electromagnetic brake, 6-signal acquisition equipment

Fig.6 Experimental system

Table. 1 The gear parameters of planetary gearbox

Gear	Sun	Ring	Planet(number)
teeth	13	92	38(3)

Note: (·) Number of planet gears in parenthesis.

Table.2 Characteristic frequencies (Hz)

Meshing frequency	Absolute rotating frequency		Fault frequency		
	Sun gear	Carrier	Sun gear	Planet gear	Ring gear
f_m=11.39 $f_s^{(r)}$	$f_s^{(r)}$	$f_c^{(r)}$=0.12 $f_s^{(r)}$	f_s=2.63 $f_s^{(r)}$	f_p=0.29 $f_s^{(r)}$	f_r=0.37 $f_s^{(r)}$

(a)

(b)

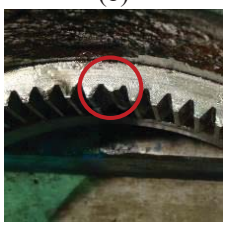

(c)

Fig. 7 Gears with manual damage. (a) sun gear fault (b) planet gear fault (c) ring gear fault.

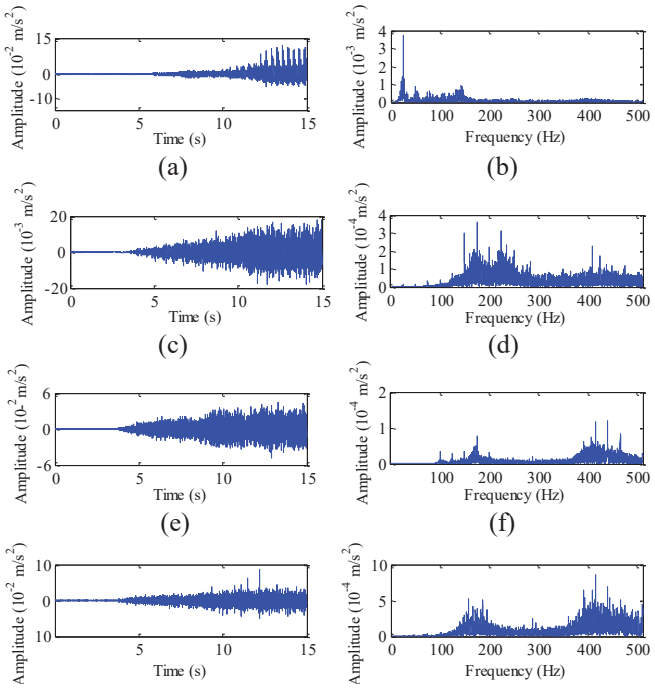

Fig. 8 The signal waveform, Fourier spectrum of one experiment for each case. (a,b) Healthy baseline, (c,d) Faulty outer race, (e,f) Faulty rolling element, (g,h) Faulty inner race.

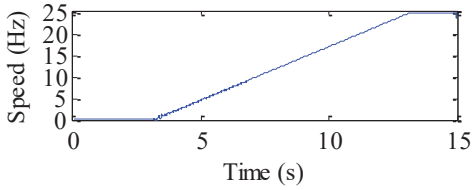

Fig. 9 Speed curve

B. Planetary gearbox fault identification under variable speed condition

The time-frequency maps are obtained by STFT as presented in Fig.10. Label normal, sun gear fault, planet gear fault, ring gear fault under variable speeds with 1,2,3,4 respectively.

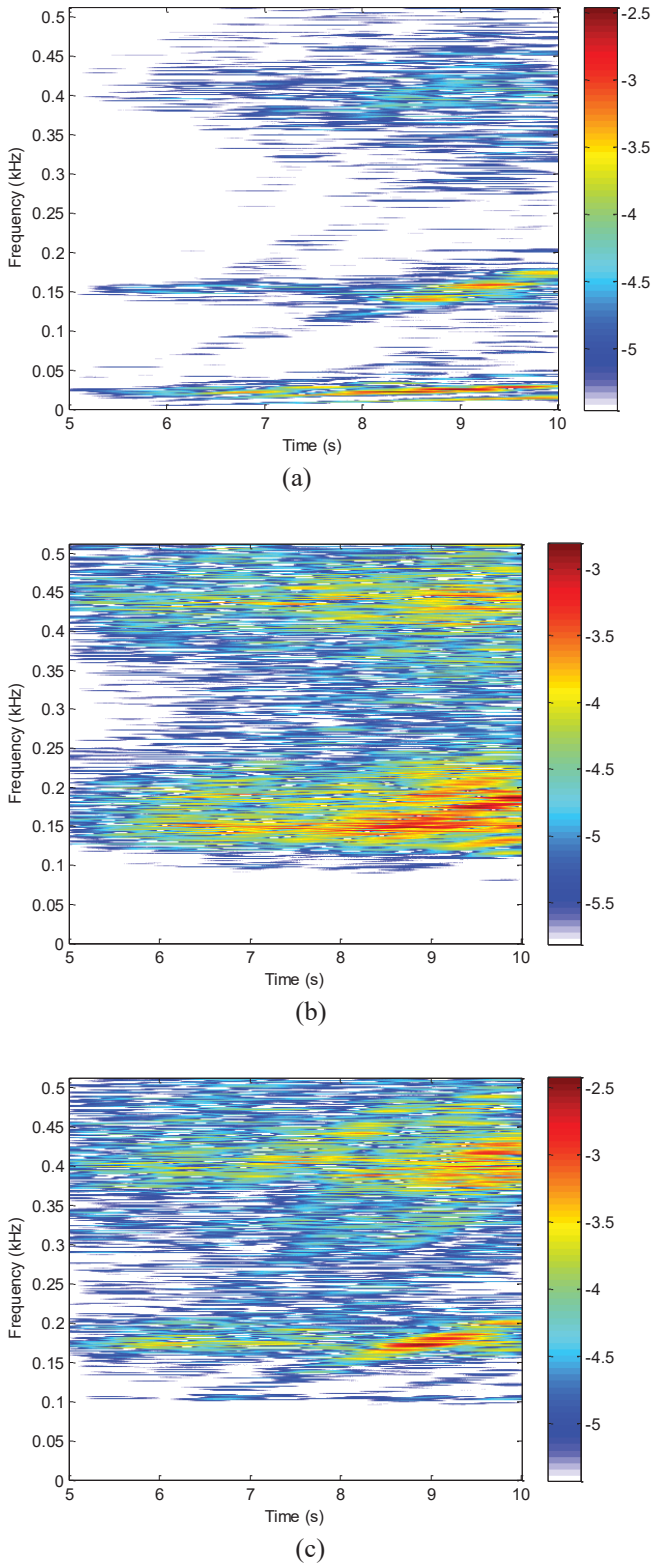

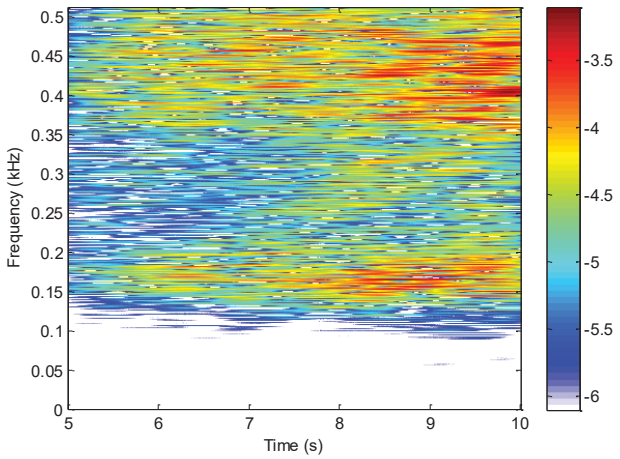

(d)

Fig.10. Time-frequency representations under different time-varying speeds. (a) normal, (b) sun gear, (c) planet gear, (d) ring gear

A CNN model is established with parameters listed in Table.3, which are taken as the same of the toolbox model, since the toolbox model is widely and effectively used for features extraction of image [19]. This study shows the trend of error rate with changeable iteration times, which is presented in Fig. 11.

Table.3 Parameters of the CNN model

Parameters	Neural network	Output maps	Kernel size	scale	Learning rate	batch	Iteration number
Value	6-5-12-5-4	6 or 12	5	2	0.1	8	100

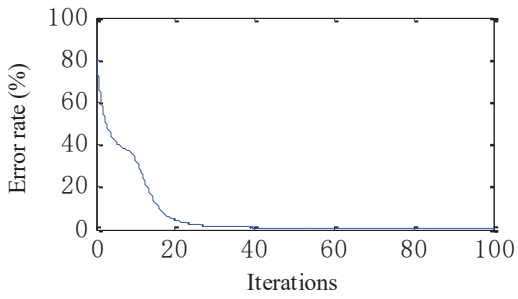

Fig.11. Error rate

Fig.11 shows that after 60 iterations, the error rate comes close to zero. All the testing samples are diagnosed correctly, which are presented in Table.4.

Table.6 Diagnosis rate of the CNN model

Signals/Label	T1	T2	A1=(T1/T2) ×100%
Sun gear fault/1	150	150	100%
Planet gear fault/2	150	150	100%
Ring gear fault/3	150	150	100%

Note: T1 - test samples classified properly, T2 - all test samples, A-identification rate

In a summary, the experiment shows that, for signals generated and collected under variable speeds, the features of time-frequency maps can be adaptively extracted by a CNN model, and the model trained with the features can diagnose the testing samples at a high accuracy. Besides, the proposed method has no limitation of time-frequency analysis methods, and is free from poor time-frequency analysis precision and pseudo interference.

V. CONCLUSIONLS

In our study, the signal can be analyzed with any time-frequency analysis method such as STFT, Wavelet Transform, Wigner-Ville distribution and empirical mode decomposition (STFT is used in our study) to obtain the corresponding time-frequency map, which is taken as the input of the model proposed based on CNN for fault diagnosis of planetary gearbox under variable speed condition. Then, the features of the map can be adaptively extracted by the CNN-based model, which are used to train the model and classified for fault diagnosis. Therefore, the model is free from poor time-frequency analysis precision and pseudo interference which are common problems in traditional time-frequency analysis. In the model, parameters of CNN are taken as the same of the toolbox model. Finally, the method is verified by an experiment. Results show that the testing samples are diagnosed at a high accuracy.

ACKNOWLEDGMENT

This work is supported by National Natural Science Foundation of China (51875034, 51475038) and doctoral research startup fund (BKY-2018-05).

REFERENCES

[1] X. H. Liang, M. J. Zuo, Z. P Feng, “Dynamic modeling of gearbox faults: A review,” Mechanical Systems and Signal Processing, vol. 98, pp. 852-876, Jan. 2018.

[2] P. D. Samuel, D. J. Pines, “A review of vibration-based techniques for helicopter transmission diagnostics,” Journal of Sound and Vibration, vol. 282, no. 1-2, pp. 475-508, Apr. 2005.

[3] C. G. Cooley, “A review of planetary and epicyclic gear dynamics and vibrations research,” Applied Mechanics Reviews, vol. 66, no. 4, pp. 1-15, Jul. 2014.

[4] Z. P. Feng, X. W. Chen, M. Liang, et al, “Time-frequency demodulation analysis based on iterative generalized demodulation for fault diagnosis of planetary gearbox under nonstationary conditions,” Mechanical Systems and Signal Processing, vol. 62-63, pp. 54-74, Oct. 2015.

[5] Z. P. Feng, X. W. Chen, M. Liang, “Joint envelope and frequency order spectrum analysis based on iterative generalized demodulation for planetary gearbox fault diagnosis under nonstationary conditions,” Mechanical Systems and Signal Processing, vol. 76-77, pp. 242-264, Aug. 2016.

[6] X. W. Chen, Z. P. Feng, “Iterative generalized time-frequency reassignment for planetary gearbox fault diagnosis under nonstationary conditions,” Mechanical Systems and Signal Processing, vol. 80, pp. 429-444, Dec. 2016.

[7] X. W. Chen, Z. P. Feng, “Time-frequency analysis of torsional vibration signals in resonance region for planetary Gearbox fault diagnosis under variable speed conditions,” IEEE Access, vol. 5, pp. 21918-21926, 2017.

[8] K. Feng, K. S. Wang, Q. Ni, et al, “A phase angle based diagnostic scheme to planetary gear faults diagnostics under non-stationary operational conditions,” Journal of Sound and Vibration, vol. 408, pp. 190-209, Nov. 2017.

[9] Y. P. Guan, M. Liang, D. S. Necsulescu, “A velocity synchro-squeezing transform for fault diagnosis of planetary gearboxes under nonstationary conditions,” Journal of Mechanical Engineering Science, vol. 231, no. 15, pp. 2868-2884, Aug. 2017.

[10] Y. Hu, X. T. Tu, F. C. Li, et al, “Joint hight-order synchro-squeezing transform and multi-taper empirical wavelet transform for fault diagnosis of wind turbine planetary gearbox under non-stationary conditions,” Sensors, vol. 18, pp. 150, Jan. 2018.

[11] L. B. Liu, X. H. Liang, M. J. Zuo, “A dependence-based feature vector and its application on planetary gearbox fault classification,” Journal of Sound and Vibration, vol. 431, pp. 192-211, Jun. 2018.

[12] Y. B. Li, G. Y. Li, Y. T. Yang, X. H. Liang, M. Q. Xu, “A fault diagnosis scheme for planetary gearboxes using adaptive multi-scale morphology filter and modified hierarchical permutation entropy,” Mechanical Systems and Signal Processing, vol. 105, pp. 319-337, Dec. 2017.

[13] Z. R. Wang, J. Wang, Y. R. Wang, “An intelligent diagnosis scheme based on generative adversarial learning deep neural networks and its application to planetary gearbox fault pattern recognition,” Neurocomputing, vol. 310, pp. 213-222, May. 2018.

[14] L. Y. Jing, M. Zhao, P. Li, X. Q. Xu, “A convolutional neural network based feature learning and fault diagnosis method for the condition monitoring of gearbox,” Measurement, vol. 111, pp. 1-10, Jul. 2017.

[15] J. Y. Jiao, M. Zhao, J. Lin, J. Zhao, “A multivariate encoder information based convolutional neural network for intelligent fault diagnosis of planetary gearboxes,” Knowledge-Based Systems, vol. 160, pp. 237-250, Jul. 2018.

[16] F. Y. Zhou, L. P. Jin, J. Dong, “Review of convolutional neural network,” Chinese journal of computers, vol. 40, no. 6, pp. 1230-1250, Jun. 2017.

[17] A. Stuhlsatz, J. Lippel, T. Zielke, “Feature extraction with deep neural networks by a generalized discriminant analysis,” IEEE Transactions on Neural Networks and Learning Systems, vol. 23, no. 4, pp. 596-608, Apr. 2012.

[18] N. T. Huang, H. J. Chen, G. W. Cai, “Mechanical fault diagnosis of high voltage circuit breakers based on variational mode decomposition and multi-layer classifier,” Sensors, vol. 1887, no. 16, pp. 1-19, Nov. 2016.

[19] Y. J. Li, T. Zhang, Introduction to deep learning and case studies. Beijing: Machinery Industry Press, 2016, pp. 221-227.